CH/π interaction between benzene and model neutral organic molecules bearing acid CH groups

Franco Ugozzoli,*[a] Arturo Arduini,[b] Chiara Massera,[a] Andrea Pochini[b] and Andrea Secchi[b]

[a] *Dipartimento di Chimica Generale e Inorganica Chimica Analitica Chimica Fisica, Università di Parma, Parco Area delle Scienze 17/A, 43100 Parma, Italy. E-mail: ugoz@unipr.it; Fax: +39 0521 905556; Tel: +39 0521 905417*

[b] *Dipartimento di Chimica Organica e Industriale, Università di Parma, Parco Area delle Scienze 17/A, 43100 Parma, Italy*

Received (in London, UK) 29th August 2002, Accepted 9th October 2002
First published as an Advance Article on the web 12th November 2002

To explore the binding properties of benzene towards small molecules bearing C–H groups with different acidities, we have undertaken *ab initio* quantum-chemical calculations, including correlation effects through Density Functional Theory methods, on the benzene–CH_3X (X = F, Cl, Br, I, CN, NO_2) adducts. Benzene acts as a Lewis base and the CH_3X molecule as a Lewis acid. The partial charge transferred from benzene to the Lewis acid is mainly confined on the X group and increases with the electron withdrawing character of X. The calculations performed on the various systems predict that two different stable structures for each adduct exist: one with C_{3v} and the other with C_s symmetry, the latter being the most stable one. A simple HOMO–LUMO model suggests that the charge is transferred from the benzene HOMO to the CH_3X LUMO and that this process is easier in the systems with C_s symmetry due to the better overlap between the frontier orbitals.

1. Introduction

In modern chemistry the non-bonding intermolecular interactions are of fundamental importance for understanding molecular recognition phenomena, biological processes and physical and chemical properties of new materials. Among them, the attractive interaction between a C–H bond and a π system, known as CH/π interaction,[1] has been invoked to explain several experimental results. Numerous examples of very short $CH\cdots C_{aromatic}$ non-bonding distances in molecules in stable conformations have been reported in the literature[2–6] as well as structural evidence of short contacts between a C–H group and a π system in a large number of organic crystals[7] and proteins.[8–10] Also, molecular recognition processes assisted by CH/π interactions are well known and documented,[11–18] however, in spite of all this evidence, few works have been devoted to understanding the physical origin of the CH/π interactions until now. Only recently the interactions between benzene and some model hydrocarbons have been investigated from the theoretical point of view.[19] In previous works we have shown that neutral macrocyclic molecules presenting intramolecular aromatic cavities are efficient hosts for neutral organic molecules possessing acid methyl groups.[20,21] The solid state structures of such complexes, obtained by single crystal X-ray diffraction, showed that the guest methyl group interacts with the aromatic surface of the host, thus leading to the hypothesis that the CH/π interaction has a stabilizing role in these systems. This experimental evidence led us to investigate from a theoretical point of view the binding mode between benzene and a series of CH_3X molecules bearing C–H groups with different acidity.

In this paper we report on the *ab-initio* theoretical calculations, carried out beyond the Hartree–Fock level including correlation effects *via* DFT calculations, on a series of complexes formed between benzene and the small molecules of the series CH_3X (X = F, Cl, Br, I, CN, NO_2). Our main purposes are: (a) to investigate the nature of the bonding between the aromatic surface of the benzene and the "acid" methyl group to elucidate an important aspect of the nature of the interactions between molecular systems and unsaturated carbon surfaces; (b) to determine the different structures of the complexes and, when possible, also the geometrical parameters sensitive to such weak interactions; (c) to evaluate the energy involved in such interactions.

2. Methodology

All the calculations reported in this work were carried out using the PC Spartan Pro release 1.05.[22] Geometry optimization calculations were performed using Density Functional methods in the perturbative Slater–Vosko–Wilk–Nusair model (SVWN) using the numerical polarization basis set SVWN/DN*.[23] The calculations were carried out on the complexes between benzene and the CH_3X (X = F, Cl, Br, I, CN, NO_2) molecules and each stationary point was characterized as a minima or a transition state by frequency calculations. Initially the geometry optimization of the isolated benzene and of the CH_3X molecules have been performed. The calculations also gave, for each molecule, the molecular electrostatic potential (MEP) plotted onto the isodensity molecular surface at 0.002 e au^{-1} [3] displayed in Fig. 1.

The MEP analysis suggested that only three different benzene–CH_3X cluster configurations (see Scheme 1) could be valid initial guesses for the geometry optimizations of the complexes: CH_3X riding on benzene (**I**), C–H bond orthogonal toward benzene (**II**) and edge-to-tail (**III**).

In **I** the plane defined by the methyl hydrogens is parallel to the benzene molecule: the system has a C_{3v} symmetry and CH_3X is "riding" on the aromatic ring. Thus the methyl

 DOI: 10.1039/b208432e

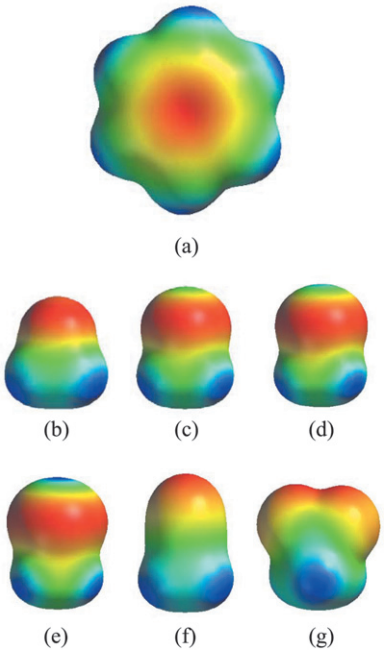

Fig. 1 Molecular Electrostatic Potential (MEP) plotted onto the molecular surfaces (the isosurface at 0.002 e au^{-1} ^{3}). Mapping colours from red (negative) to blue (positive). (a) Benzene (MEP values from −20.6 to 15.3 kcal mol^{-1}), (b) CH_3F (−26.2, 20.7), (c) CH_3Cl (−19.8, 23.7), (d) CH_3Br (−18.8, 24.8), (e) CH_3I (−21.6, 21.1) (f) CH_3CN (−45.5, 31.8), (g) CH_3NO_2 (−35.8, 34.2).

molecular surface, where the MEP is positive, is just faced on the benzene nucleus where the MEP is negative.

In **II** only one methyl hydrogen points towards the barycentre of the benzene and the plane defined by HCX is orthogonal to it, resulting in a system with C_s symmetry. In this cluster configuration, two weak attractive interactions can cooperate simultaneously: one between the methyl hydrogen atom (where the MEP is positive) pointing toward the barycentre of benzene and the barycentre itself (where the MEP is negative) and one between the X group (were the MEP is negative) and one hydrogen atom of the ring (where the MEP is positive).

In **III** the C–X bond is initially aligned with a benzene C–H bond. In the benzene nitromethane complex the CNO_2 group is placed coplanar to the aromatic ring with the nitro group close to two adjacent benzene hydrogen atoms.

As significant geometrical parameters potentially sensitive to the strength of the intermolecular interactions were chosen: (a) the distance between the CH_3 carbon atom and the barycentre of the benzene, namely $\boldsymbol{R}$ in **I** and $\boldsymbol{R_1}$ in **II**; (b) the distance between the hydrogen pointing towards the barycentre of the benzene and the barycentre itself, $\boldsymbol{R_2}$ in **II**; (c) the angle between the C–X bond and the line parallel to the benzene group and lying on the mirror plane of the complex, $\boldsymbol{\alpha_1}$ in **II**, and the angle C–H···barycentre $\boldsymbol{\alpha_2}$ in **II**. Since the rearrangement of charge which accompanies the complex formation is an important indicator of the nature and of the strength of the binding, the charge shift $\boldsymbol{q}$, namely the charge transferred from benzene to the CH_3X molecule, has been calculated starting from the electrostatic charges.

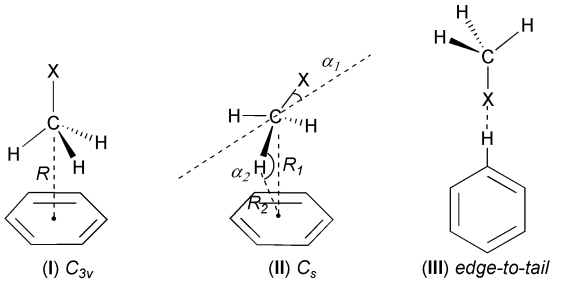

Scheme 1

3. Results and discussion

3.1 Individual molecules

Results obtained at the SVWN/DN* level for the individual molecules after geometry optimizations are collected in Table 1. The variations in the bond distances and angles in the individual molecules during the complex formation are small in the whole series of complexes. The C–C and C–H bond lengths in benzene change a maximum of 0.002 Å and the increases in the C–X and C–H bond distances in the halogen series do not exceed 0.003 and 0.004 Å, respectively. On the contrary, in the CH_3CN and CH_3NO_2 complexes the bond distances decrease. The maximum variations are observed for the C–N and C–H bond distances in the case of nitromethane (0.006 Å).

The HCX bond angle generally increases in the complexes with C_{3v} symmetry (the shift ranges from 0.27 to 1.44°) but, on the contrary, in the complexes with C_s symmetry it decreases for the hydrogen atom pointing towards the barycentre of the benzene (the maximum shift of −1.38° is observed for nitromethane) indicating that in this cluster configuration the attractive interactions between the benzene and the CH_3X molecule also involve the X group other than the methyl group.

3.2 Clusters with C_{3v} symmetry

Table 2 reports the results obtained from the geometry optimization starting with the methyl group "riding" on benzene in the C_{3v} symmetry.

In this cluster configuration all the three "acid" hydrogens of the methyl group interact simultaneously with benzene giving rise to the so called CH_3/π interaction.

At the SVWN/DN* level all the complexes exhibit modest binding: the interaction energies range from 73 to 92% of the interaction energy of the water dimer (5.0 kcal mol^{-1}).[24] The aromatic ring acts as a Lewis base and transfers a partial charge $\boldsymbol{q}$ to the CH_3X molecule (the Lewis acid); $\boldsymbol{q}$ is mainly confined on the X group and the highest $\boldsymbol{q}$ values are observed, as expected, for the cyano and nitro groups. Among the halides there is no evidence of linear correlation between $\boldsymbol{q}$ and the electron withdrawing character of X.

In Figs. 2 and 3 the energy values, plotted against the equilibrium distance $\boldsymbol{R}$ and the transferred charge $\boldsymbol{q}$, respectively, show that the stability of the system increases as $\boldsymbol{q}$ increases, with the anomalous case of the benzene CH_3Br complex. In conclusion, in this cluster configuration the CH/π interaction seems to have a significant electrostatic component, but the non-linear correlation between $-\boldsymbol{E}$ and $\boldsymbol{q}$ suggests that dispersion forces also contribute significantly. In fact, a scan of $\boldsymbol{E}$ as a function of $\boldsymbol{R}$ shows that a substantial attraction exists also at larger intermolecular $\boldsymbol{R}$ values indicating that these complexes

Table 1 Bond distances (Å) in the individual molecules after geometry optimization

Benzene	C–C 1.387	C–H 1.097	
CH_3F	C–F 1.376	C–H 1.103	
CH_3Cl	C–Cl 1.767	C–H 1.098	
CH_3Br	C–Br 1.983	C–H 1.096	
CH_3I	C–I 2.149	C–H 1.096	
CH_3CN	C–C 1.437	C–N 1.160	C–H 1.102
CH_3NO_2	C–N 1.474	N–O 1.220	C–H 1.099

Table 2 Benzene–CH_3X adducts in the C_{3v} symmetry, $\boldsymbol{E}$ = binding energy, $\boldsymbol{R}$ see Scheme 1, $\boldsymbol{q}$ = charge transferred from benzene to the CH_3X molecule

CH_3X riding on benzene (C_{3v} symmetry)			
X	E/kJ mol^{-1}	R/Å	q/e
F	−15.195	3.308	0.005
Cl	−15.823	3.286	0.006
Br	−14.944	3.291	0.011
I	−15.949	3.267	0.009
CN	−18.753	3.262	0.022
NO_2	−19.256	3.299	0.030

are stabilized by long-range interactions such as electrostatic and dispersion rather than short-range interactions. The $\boldsymbol{R}$ values are uncorrelated to the binding energy so that it is not a "good" geometrical parameter being insensitive to the strength of the attraction.

3.3 Clusters with C_s symmetry

The results obtained from the geometry optimization starting with one methyl hydrogen pointing towards the barycentre of benzene are reported in Table 3.

The complexes in this symmetry exhibit the highest attraction: $\boldsymbol{E}$ becomes more negative and ranges from 79 to 143% of the interaction energy of the water dimer. A partial charge $\boldsymbol{q}$ is shifted from benzene to the CH_3X molecule and segregated on the X group. Such an increase in the complex stability, with respect to that predicted for the complexes with C_{3v} symmetry, can be explained on the basis of a double electrostatic attractive interaction of "acid–base" type: one "acid" hydrogen of the methyl group interacts with the negative charge concentrated on the baricentre of benzene through a simple CH/π interaction while the negative charge concentrated on the X group interacts with the partially positive hydrogens of the benzene. This double-interaction model is supported by the variation of the X–C–H bond angle, which, as stated above, increases during the formation of the complexes with C_{3v} symmetry, whereas it decreases by −1.38° in the complexes with C_s symmetry.

In Fig. 4 the binding energy values are plotted together with the transferred charges $\boldsymbol{q}$ for the whole series of adducts; the binding increases when $\boldsymbol{q}$ increases, showing an almost linear correlation between $-\boldsymbol{E}$ and $\boldsymbol{q}$ from benzene CH_3Br to benzene CH_3NO_2 suggesting that the electrostatic component of the interactions is stronger in this cluster configuration. The high attraction between benzene and CH_3F is surprising and suggests that also in this cluster symmetry the dispersion interaction contributes significantly to the binding.

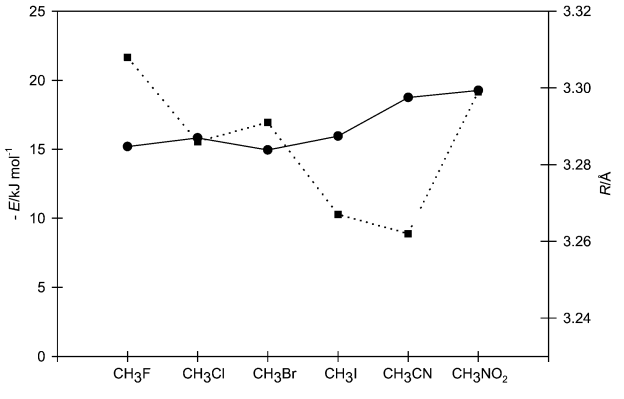

Fig. 2 Binding energy $-E$ (—) and R (···) along the series of adducts in the C_{3v} symmetry.

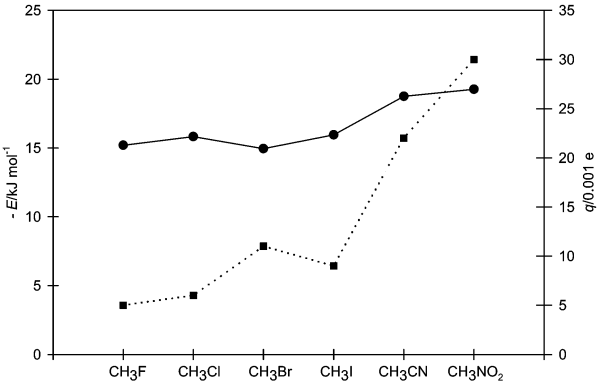

Fig. 3 Binding energy $-E$ (—) and q (···) along the series of adducts in the C_{3v} symmetry.

On the contrary none of the geometrical parameters, $\boldsymbol{R_1}$, $\boldsymbol{R_2}$, $\boldsymbol{\alpha_1}$ and $\boldsymbol{\alpha_2}$ can account for the strength of the binding. For instance $\boldsymbol{R_1}$ is totally uncorrelated to $-\boldsymbol{E}$ (see Fig. 5). This behaviour is not surprising, but, on the contrary, it supports the hypothesis that the complex is stabilized through a double interaction whereas the $\boldsymbol{R_1}$ values could account, at maximum, only for one of them.

The structure of the benzene CH_4 complex with C_s symmetry has also been optimized with the DFT method in the SVWN/DN* model. The calculated binding energy ($\boldsymbol{E}$ = −10.042 kJ mol^{-1}) allows us to estimate the contribution of the dispersion interactions to the total binding along the series of the complexes with C_s symmetry (the most stable ones): the contribution of the dispersion is substantial and ranges from 60% in the benzene CH_3F complex to 33% in the benzene CH_3NO_2 complex.

3.4 Edge-to-tail clusters

In this cluster configuration the strength of the binding shows its lowest intensity: −3.60, −7.242, −5.149, −0.879, −3.935, −8.539 kJ mol^{-1} along the series; the equilibrium geometries never correspond to a true edge-to-tail configuration. The vibrational frequencies, calculated to characterize the stationary point in the potential energy surface, lead to imaginary values for all the complexes with the exception of benzene–CH_3NO_2, the most stable one in this cluster configuration. However it must be emphasized that in this case the CH/π interaction does not occur since the NO_2 group is linked to the aromatic ring through the two hydrogen bonds shown in Fig. 6. The H···O contacts are 2.64 and 2.512 Å, respectively.

3.5 HOMO and LUMO

Geometrical optimizations of the isolated molecules *in vacuo* using DFT calculations at the SVWN/DN* level gave the energy of the highest occupied molecular orbital (HOMO) of

Table 3 Benzene–CH_3X adducts in the C_{3v} symmetry, $\boldsymbol{E}$ = binding energy, $\boldsymbol{R}_1$, $\boldsymbol{R}_2$, $\boldsymbol{\alpha}_1$ and $\boldsymbol{\alpha}_2$ see Scheme 1, $\boldsymbol{q}$ = charge transferred from benzene to the CH_3X molecule

CH_3X orthogonal to benzene (C_s symmetry)						
X	E/kJ mol^{-1}	q/e	R_1/Å	R_2/Å	α_1/°	α_2/°
F	−16.577	0.012	3.413	2.351	0.42	160.72
Cl	−20.051	0.003	3.481	2.423	−7.55	160.42
Br	−18.167	0.008	3.414	2.338	−0.14	165.57
I	−20.009	0.012	3.393	2.313	5.94	167.69
CN	−24.572	0.021	3.275	2.418	−6.52	133.16
NO_2	−30.014	0.025	3.337	2.356	−13.88	146.90

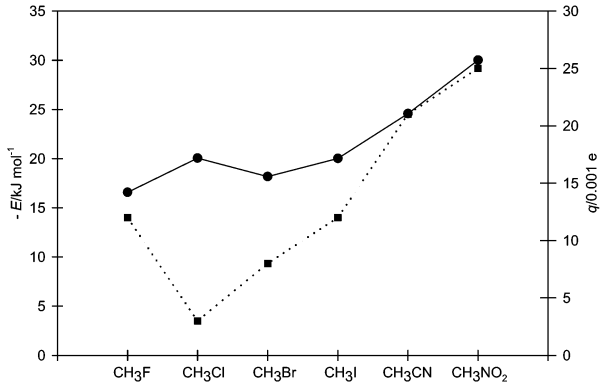

Fig. 4 Binding energy $-E$ (—) and q ($\cdots$) along the series of adducts with C_s symmetry.

benzene (-636.55 kJ mol^{-1}) and of the lowest unoccupied molecular orbital (LUMO) of the CH_3X molecules whose values are reported in Table 4.

The analysis of the HOMO–LUMO separation and of the symmetry of the frontier orbitals helps us to understand how the electrostatic charge is transferred from benzene to the CH_3X molecule. Fig. 7 shows that, except for the case of the benzene–CH_3CN complex, the energy separation between the HOMO of benzene and the LUMO of CH_3X decreases linearly along the series from CH_3F to CH_3NO_2.

A linear increase of $\boldsymbol{q}$ along the same series of complexes (both in C_s and C_{3v} cluster configurations) could thus be expected. On the contrary, an abrupt increase of the $\boldsymbol{q}$ value is always observed in the complexes with CH_3CN and CH_3NO_2. Such a trend can be explained by looking at the pivotal role of the HOMO–LUMO overlap in all the complexes; Figs. 8 and 9 show the overlap between the limit surfaces of the frontier orbitals in the C_{3v} and C_s cluster configurations, respectively.

Considering the complexes with C_{3v} symmetry, when X is a halide the overlap between the HOMO and the LUMO results in a partial reciprocal cancellation between the wave functions and this hinders the charge transfer. On the contrary in the case of CH_3CN and CH_3NO_2 complexes the overlap brings a summation between the frontier orbitals with identical sign, thus justifying the observed abrupt increase of the charge transferred from the base to the acid compound.

The reciprocal orientation of the frontier orbitals is more favourable in the series of complexes with C_s symmetry, and the overlap also becomes constructive (even if a little bit of cancellation still remains) for the complexes with CH_3Cl, CH_3Br and CH_3I. However it is worth noticing that also in this configuration the overlap between HOMO and LUMO

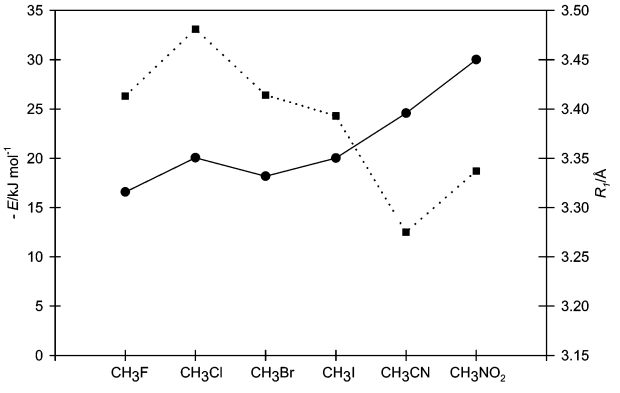

Fig. 5 Binding energy $-E$ (—) and R_1 ($\cdots$) along the series of adducts with C_s symmetry.

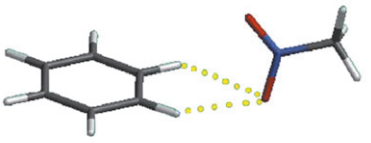

Fig. 6 Optimized structure of the benzene CH_3NO_2 complex in the edge-to-tail configuration.

increases dramatically for the complexes with CH_3CN and CH_3NO_2 resulting in the correlated increase of the charge transfer.

3.6 Binding and acidity

The binding energies of the complexes have been compared with the Lewis acidities of the CH_3X molecules to evidence a possible correlation between these properties. A reliable indicator for the acidity of a hydrogen atom in a molecule is the highest value of the MEP in correspondence to the acid H-atom.[25]

In our case the maximum values calculated on the molecular isosurface at 0.002 e au^{-13} around the methyl group are 86.7, 99.2, 103.8, 88.3, 133.1, 143.2 kJ mol^{-1} along the series from CH_3F to CH_3NO_2.[26] In Fig. 10 the $MEP_{(max)}$ values are plotted together with the binding energies in both the cluster configurations. As a general trend, the binding energy increases with the acidity (except for the CH_3I complex) and the best correlation is obtained for complexes with C_{3v} symmetry, (the less stable) rather than for those with C_s symmetry. This behaviour however is not surprising considering that in complexes with C_{3v} symmetry the only active interaction is the CH/π one, which reasonably depends linearly on the acidity. In the case of C_s symmetry however, since the interaction is not a pure CH/π but a second electrostatic force cooperates with it to enhance the binding, a linear dependence between the binding energy and the acidity of the CH_3X molecule is partially prevented.

3.7 Accuracy of the results

Since no experimental binding energies in the gas phase are available so far, the accuracy of the obtained results can only be estimated by comparison with theoretical results obtained by high-level *ab initio* calculation. In a very recent paper[27] the intermolecular interaction energies were calculated for the benzene CH_4 and benzene CH_3Cl complexes using extrapolated MP2[28,29] interaction energies at the basis set limit and CCSD(T) correction terms.[30,31] The calculated benzene CH_4 interaction energy is -6.069 kJ mol^{-1} and that for benzene CH_3Cl is -12.56 kJ mol^{-1}. These results compared to the corresponding ones obtained by us indicate that the equilibrium geometries are almost identical for the two methods and that the DFT method in the SVWN/DN* model overestimates the binding by almost 60% for both the complexes. However in the same paper are also reported the binding energies obtained by MP2/6-311G** *ab initio* calculations which show that on

Table 4 Energy values of the LUMO in the CH_3X molecules

X	LUMO's energy/kJ mol^{-1}
F	58.61
Cl	−47.38
Br	−120.21
I	−195.29
CN	−53.53
NO_2	−327.61

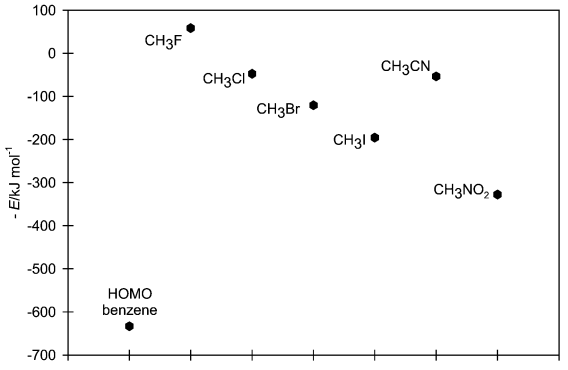

Fig. 7 Energy levels of the HOMO of benzene and of the LUMO of the CH_3X molecules.

the contrary, with this basis set the binding is underestimated by 45 and 30% (−3.35 and −8.79 kJ mol^{-1} for the methane and chloromethane complexes, respectively) with respect to the MP2 basis set limit and CCSD(T) correction terms. This

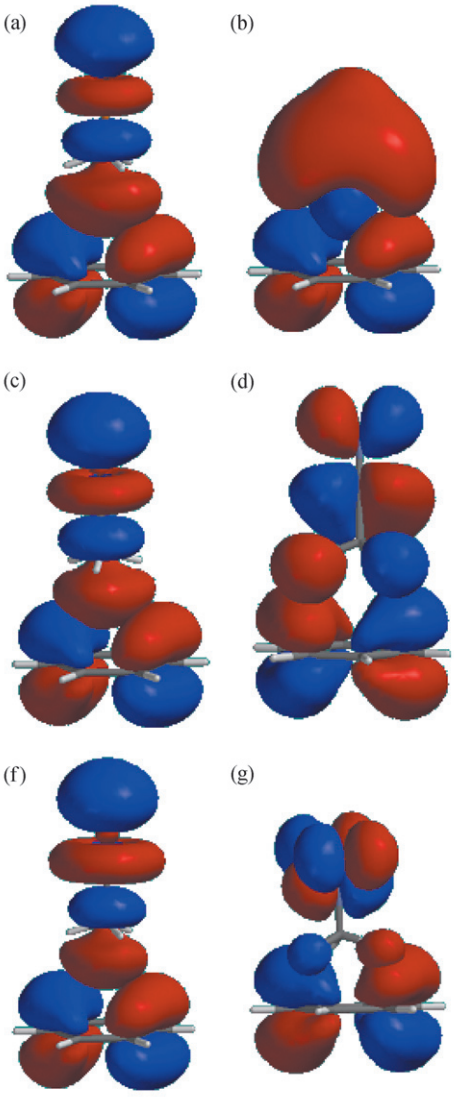

Fig. 8 Perspective view of the overlap between frontiers orbitals (isosurfaces at 0.032 e au^{-13}) in the C_{3v} adducts of benzene with (a) CH_3F, (b) CH_3I, (c) CH_3Cl, (d) CH_3CN, (e) CH_3Br and (f) CH_3NO_2, respectively.

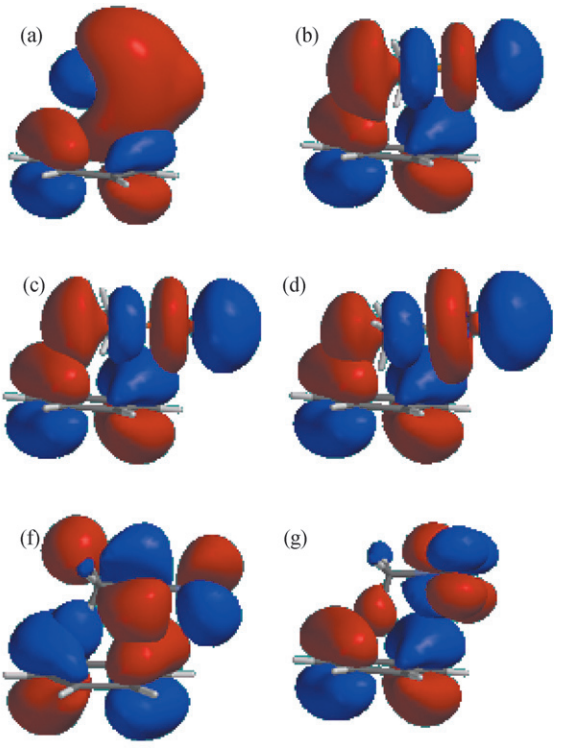

Fig. 9 Perspective view of the overlap between frontiers orbitals (isosurfaces at 0.032 e au^{-13}) in the C_s adducts of benzene with (a) CH_3F, (b) CH_3I, (c) CH_3Cl, (d) CH_3CN, (e) CH_3Br and (f) CH_3NO_2, respectively.

indicates that the calculations strongly depend on the basis set and that the calculations proposed by us can lead to an accuracy of the geometries comparable to that obtained with the MP2/6-311G** method, although in our case the energies are overestimated rather than underestimated.

Conclusions

DFT calculations at the SVWN/DN* level predict that benzene can bind small CH_3X molecules bearing acid CH groups with different acidities. Benzene acts as a Lewis base and the CH_3X molecule as a Lewis acid. Two different cluster configurations are possible, one with C_{3v} and the other (the most stable one) with C_s symmetry. In the first case only the CH/π interaction, which has a significant electrostatic component, is responsible for the binding; in complexes presenting C_s

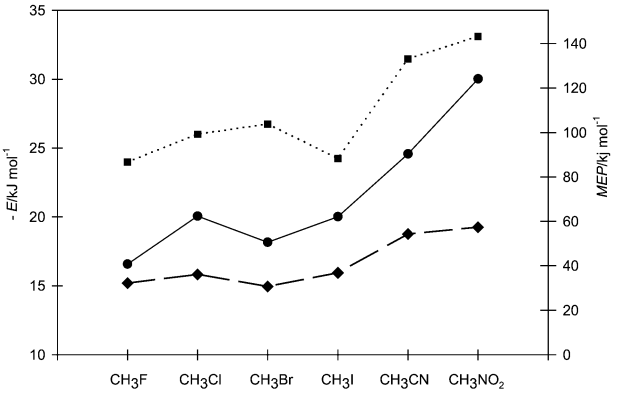

Fig. 10 $MEP_{(max)}$ values (kJ mol^{-1}) (···) on the isolated CH_3X molecules and binding energies $-E$ (kJ mol^{-1}) for the complexes with C_s (—) and C_{3v} (---) symmetry.

symmetry two attractive interactions enhance the stability of the complexes: beside the CH/π one, an electrostatic interaction also exists, namely between the X group (on which lies an excess of negative charge) and one aromatic hydrogen atom (on which an excess of positive charge is localized). A physical route through which the charge is transferred from the Lewis base to the Lewis acid has been proposed, considering the HOMO–LUMO separations and the different overlap between frontier orbitals in the two possible cluster configurations.

Acknowledgements

We thank Prof. R. Cammi for the stimulating discussion during the preparation of the manuscript and the Ministero dell'Istruzione, dell'Università e della Ricerca (MIUR) "Supramolecular Devices" project for financial support.

References

1 (*a*) M. Nishio, M. Hirota and Y. Umezawa, *The CH/π Interaction*, Wiley-VCH, New York, 1998; (*b*) O. Takahashi, Y. Kohno, S. Iwasaki, K. Saito, M. Iwaoka, S. Tomoda, Y. Umezawa, S. Tsuboyama and M. Nishio, *Bull. Chem. Soc. Jpn.*, 2001, **74**, 2421; (*c*) O. Takahashi, S. Tsuboyama, Y. Umezawa, K. Honda and M. Nishio, *Tetrahedron*, 2000, **56**, 6185; (*d*) Y. Umezawa, S. Tsuboyama, H. Takahashi, J. Uzawa and M. Nishio, *Bioorg. Med. Chem.*, 1999, **7**, 2021; (*e*) R. E. Grillard, F. M. Raymo and J. F. Stoddart, *Chem. Eur. J.*, 1997, **3**, 1933; (*f*) P. Timmermann, W. Verboom and D. N. Reinhoudt, *Tetrahedron*, 1996, **52**, 2663; (*g*) For a comprehensive literature list see http://www.tim.hi-ho.ne.jp/dionisio/.
2 Y. Iitaka, Y. Kodama, K. Nishihata and M. Nishio, *J. Chem. Soc., Chem. Commun.*, 1974, 389.
3 Y. Kodama, K. Nishihata, M. Nishio and Y. Iitaka, *J. Chem. Soc., Perkin Trans. 2*, 1976, 1490.
4 Y. Kodama, S. Zushi, K. Nishihata, M. Nishio and J. Uzawa, *J. Chem. Soc., Perkin Trans. 2*, 1980, 1306.
5 M. Hirota, T. Sekiya, K. Abe, H. Tashiro, M. Karatsu, M. Nishio and E. Osawa, *Tetrahedron*, 1983, **39**, 3091.
6 Y. Nakai, G. Yamamoto and M. Oki, *Chem. Lett.*, 1987, 89.
7 Y. Umezawa, S. Tsuboyama, H. Takahashi, J. Uzawa and M. Nishio, *Tetrahedron*, 1999, **55**, 10 047.
8 F. A. Quiocho and N. K. Vyas, *Nature*, 1984, **310**, 381.
9 N. K. Vyas, M. N. Vyas and F. A. Quiocho, *Nature*, 1987, **327**, 635.
10 N. K. Vyas, M. N. Vyas and F. A. Quiocho, *Science*, 1988, **242**, 1290.
11 G. D. Andreetti, A. Pochini and R. Ungaro, *J. Chem. Soc., Chem. Commun.*, 1979, 1005.
12 G. D. Andreetti, O. Ori, F. Ugozzoli, C. Alfieri, A. Pochini and R. Ungaro, *J. Inclusion Phenom.*, 1988, **6**, 523.
13 E. Dalcanale, P. Soncini, G. Bacchilega and F. Ugozzoli, *J. Chem. Soc., Chem. Commun.*, 1989, 500.
14 K. Kobayashi, Y. Asakawa, Y. Kato and Y. Aoyama, *J. Am. Chem. Soc.*, 1992, **114**, 10 307.
15 K. Kobayashi, Y. Asakawa, Y. Kikuchi, H. Toi and Y. Aoyama, *J. Am. Chem. Soc.*, 1993, **115**, 2648.
16 D. B. Amabilino, P. R. Ashton, C. L. Brown, E. Cordova, L. A. Godinez, T. T. Goodnow, A. E. Kaifer, S. P. Newton, M. Pietraszkiewicz, D. Philp, F. M. Raymo, A. S. Reder, M. T. Rutland, A. M. Z. Slawin, N. Spencer, J. F. Stoddart and D. J. Williams, *J. Am. Chem. Soc.*, 1995, **117**, 127.
17 R. Ballardini, V. Balzani, A. Credi, C. L. Brown, R. E. Gillard, M. Montalti, D. Philp, J. F. Stoddart, M. Venturi, A. J. P. White, B. J. Williams and D. J. Williams, *J. Am. Chem. Soc.*, 1997, **119**, 12 503.
18 M. Asakawa, P. R. Ashton, W. Hayes, H. M. Janssen, E. W. Meijer, S. Menzer, D. Pasini, J. F. Stoddart, A. J. P. White and D. J. Williams, *J. Am. Chem. Soc.*, 1998, **120**, 920.
19 (*a*) S. Tsuzuki, K. Honda, T. Uchimaru, M. Mikami and K. Tanabe, *J. Am. Chem. Soc.*, 2000, **122**, 3746; (*b*) S. Tsuzuki, K. Honda, T. Tadafumi, M. Mikami and K. Tanabe, *J. Phys. Chem. A*, 2002, **106**, 4423.
20 A. Arduini, F. F. Nachtigall, A. Pochini, A. Secchi and F. Ugozzoli, *Supramol. Chem.*, 2000, **12**, 273.
21 A. Arduini, G. Giorgi, A. Pochini, A. Secchi and F. Ugozzoli, *Tetrahedron*, 2001, **57**, 2411.
22 Wavefunction, Inc., 18401 Von Karman Avenue, Suite 370, Irvine, CA 92612, USA, 2001.
23 Numerical polarization basis sets in the SVWN (Slater, Vosko, Wilk, Nusair) model. Review of density functional theory (*a*) R. O. Jones and O. Gunnarssons, *Rev. Mod. Phys.*, 1989, **61**, 689R. G. Parr and W. Yang, *Density Functional Theory of Atoms and Molecules*, Oxford Univ. Press, Oxford, 1989; (*b*) J. K. Labanowky and J. W. Andzelm, ed. *Density Functional Methods in Chemistry*, Springer Verlag, New York, 1991.
24 P. O. Widmark, P. A. Malmqvist and B. O. Roos, *Theor. Chim. Acta*, 1990, **79**, 290.
25 J. A. Platts, *Phys. Chem. Chem. Phys.*, 2000, **2**, 973.
26 A similar trend has been calculated and experimentally measured for the complete deprotonation of CH_3F, CH_3Cl, CH_3CN, CH_3NO_2, see I. F. Tupisyn and A. S. Popov, *Russ. J. Gen. Chem.*, 2001, **71**, 89 (translated from *Zh. Obshch. Khim*, 2001, **71**, 97) and references therein.
27 S. Tsuzuki, K. Honda, T. Uchimaru, M. Mikami and K. Tanabe, *J. Phys. Chem. A*, 2002, **106**, 4423.
28 C. Møller and M. S. Plesset, *Phys. Rev.*, 1934, **46**, 618.
29 M. Head-Gordon, J. A. Pople and M. J. Frisch, *Chem. Phys. Lett.*, 1988, **153**, 503.
30 J. A. Pople, M. Head-Gordon and K. Raghavachari, *J. Chem. Phys.*, 1987, **87**, 5968.
31 G. E. Scuseria and H. F. Schafer, *J. Chem. Phys.*, 1989, **90**, 3700.